

The Ratio of  $D^0$  and  $D^+$  Lifetimes from their Semileptonic Decays \*

G. J. Donaldson  
 Stanford Linear Accelerator Center  
 Stanford University, Stanford, California 94305

The conventional expectation<sup>1</sup> for the decays of D mesons assumes that the charm quark decays in the presence of light, spectator quarks and thus the lifetimes of both charged and uncharged states are equal. In this article, I present evidence from DELCO (at SPEAR) that the D lifetimes are quite different for neutral and charged mesons,<sup>2</sup> and review the results which have also become available from other experiments.

In  $e^+e^-$  annihilations, current experiments do not measure the D lifetime directly. The copious production of  $D\bar{D}$  pairs at the  $\psi'$  instead allows a determination of the semileptonic branching fraction which must be combined with theoretical input to calculate the total lifetime. The  $\Delta I = 0$  nature of the  $c \rightarrow sev$  transition is such that one expects equal rates for each possible semileptonic transition:

$$(1) \quad \Gamma(D^0 \rightarrow K^- e^+ \nu) = \Gamma(D^+ \rightarrow \bar{K}^0 e^+ \nu)$$

$$(2) \quad \Gamma(D^0 \rightarrow \bar{K}^0 \pi^- e^+ \nu) = \Gamma(D^+ \rightarrow K^- \pi^+ e^+ \nu) \quad \text{etc.,}$$

and the sum over all channels implies that

$$(3) \quad \Gamma(D^0 \rightarrow Xev) = \Gamma(D^+ \rightarrow Xev)$$

This, together with the branching ratio definition

$$(4) \quad \text{br}(D \rightarrow Xev) \equiv \frac{\Gamma(D \rightarrow Xev)}{\Gamma(D \rightarrow \text{all})}$$

gives the ratio of lifetimes:

$$(5) \quad \frac{\tau(D^+)}{\tau(D^0)} = \frac{\text{br}(D^+ \rightarrow Xev)}{\text{br}(D^0 \rightarrow Xev)}$$

Experimentally, the ratio of lifetimes is obtained by measuring the right hand side of this equation.

There are a variety of techniques in  $e^+e^-$  annihilation which could be used to determine the branching fractions  $b^0$  and  $b^+$ . ( $b^0 = \text{br}(D^0 \rightarrow Xev)$ )

\*Work supported in part by the National Science Foundation, and in part by the Department of Energy under contract number DE-AC03-76SF00515.  
 (Invited talk at the Orbis Scientiae, Coral Gables, Florida, January 14-17, 1980.)

and  $b^+ = \text{br}(D^+ \rightarrow Xev)$ ). The fundamental question that DELCO addresses is "What fraction of the charm semileptonic decays come from  $D^0\bar{D}^0$  versus  $D^+\bar{D}^-$ ?" We use events of the reaction  $e^+e^- \rightarrow \psi(3772) \rightarrow D\bar{D}$  to compare the rate of observing a "1e" event from  $D\bar{D}$  decay with the rate of observing a "2e" event from  $D\bar{D}$  decay. (A "1e" or "2e" event is a multi-prong hadron event containing 1 or 2 electrons respectively). The former is proportional to a combination of  $b^0$  and  $b^+$ , the latter is proportional to  $(b^0)^2$  and  $(b^+)^2$ . Another technique<sup>3)</sup> uses a fully reconstructed hadronic decay ("tagged D") identifying the charge state of the  $D\bar{D}$  pair to count the semileptonic decays of the other D. This is the method reported by the Mark II group at SPEAR. Furthermore, there is the possibility<sup>4)</sup> of using the energy dependence of the multi-prong electron cross section which changes as the neutral to charged fraction of D's varies with energy. Finally, one could use a soft  $\pi^+$  tag in  $D^{*+}\bar{D}^-$  events to identify the presence of a  $D^0$  and  $D^-$ . These last two techniques suffer from ambiguities in the production mechanisms for the  $D\bar{D}$  pair, making difficult a precise determination of the charge nature of the initial state. For this reason, the data used in this analysis covers only from  $\psi$  decays where the D production is well known, and the experimental acceptance can be reliably calculated.

The DELCO apparatus, (Fig. 1) has been described in detail elsewhere<sup>5</sup>, and only a brief account appears herein. Particles emanating from the interaction point first traverse a set of cylindrical proportional chambers, and then pass through an atmospheric ethane Cherenkov counter into a lead-scintillator sandwich of time-of-flight (and shower) counters. Their final positions are recorded by magnetostrictive wire spark chambers. The strength of this detector lies in its very good electron identification and hadron rejection so that the multi-prong events containing 1 or 2

electrons at the  $\psi'$  have a very high probability of originating in charm decays.

The event selection provides two fundamental samples which are similar in nature (but different in the requirement details.) The 1e sample contains events having 1 electron, and  $\geq 2$  additional charged tracks, where the electron is defined to be a track passing through a latched Cherenkov cell (one of 12 such cells). The 2e sample contains events having 2 electrons and  $\geq 1$  "unambiguous non-electron". In this case, the electrons are required to be the only tracks in the cell, and an "unambiguous non-electron" refers to a track having  $p > 200$  MeV (Ch. threshold) passing through a Cherenkov cell which did not fire. The 2e sample has a number of potential backgrounds which are dealt with both by a visual scan and by cuts on the topological and kinematic properties of the events. (The 1e sample is discussed in detail in Ref. 6.) These are shown in Table I. Even after the above requirements it is not possible to tell on an event-by-event basis which are background and which signal. However, a comparison of the electron momentum spectrum from the 2e sample with the fitted shape obtained from the much higher statistics of the 1e sample demonstrates that the electrons in the 2e sample have the correct momentum spectrum. This is shown in Figure 2 for those electrons whose momentum is well-measured.

There are, of course, residual backgrounds remaining in the 2e sample described above: The most important of these are as follows: 1) non-charm actual 2e events - such as  $2\gamma$  processes (Fig 3) and  $\eta$  Dalitz pairs, 2) 1 real electron (from a D or  $\tau$  decay - or  $\gamma$  conversion) plus 1 spurious electron from hadron misidentification; and 3) 2 spurious electrons.

Table I

<u>Backgrounds to 2e Sample</u>	<u>Suppression Method</u>
1) $e^+e^- \rightarrow e^+e^- \gamma$	hand-scan
2) $e^+e^- \rightarrow \text{hadrons}, \gamma \rightarrow e^+e^-$	} candidate electron tracks must have hits in the inner PWC planes.
3) false signatures	
4) non-charm decays to electrons	electron must be reconstructed as originating at interaction point.
5) two photon processes ( $e^+e^- \rightarrow eeee, ee\mu\mu$ )	require $P_e < 1 \text{ GeV}$ and $\Delta\phi_{ee} < 160^\circ$ ; $\phi_{ee}$ is defined in the azimuthal projection
6) $\pi^0, \eta$ Dalitz decays	require $M_{ee} > M_{\pi^0}$ and $\Delta\phi_{ee} > 5^\circ$
7) $\psi' \rightarrow \psi' \rightarrow \psi \pi^+ \pi^-$ $\downarrow$ $e^+e^-$	require $\Delta\phi_{ee} < 150^\circ$ for 4 track events

The calculation of these residual backgrounds is the most difficult and complicated aspect of the analysis. The basic strategy is to use the data below the  $\psi''$  to identify and study background processes, and then calculate how many background events should be present in the  $\psi''$  sample. To do this, we divide the data into three regions: a)  $\psi''$  (where the events are from both charm decays and background) b)  $\psi + \psi'$ , where the very large value of R enhances those backgrounds which are intrinsic to hadronic events, and c) between the  $\psi$  and  $\psi'$ , where a substantial accumulation of running time (acquired while mapping the  $\tau$  threshold region) produced a large number of hadronic events of non-resonant origin.

In each of these regions a small number of two-photon events are predicted by a Monte Carlo calculation<sup>7</sup>, and subtracted. Events at the  $\psi(3100)$  are studied to determine the misidentification probability for a hadron within a singly-occupied Cherenkov cell ( $\sim 1.8 \times 10^{-3}$ ). We then use events in the 1e sample to calculate the 2e background (in all three regions) by randomly assigning an extra Cherenkov tag to eligible hadron tracks at the appropriate rate, and subjecting the resulting events to identical requirements to the actual 2e data sample.

Using the 1e sample in this manner guarantees that the proper mixture of electrons from charm and  $\tau$  decays (as well as background e's) is automatically included. After subtracting off these background events, there are still events remaining at the  $\psi$  and  $\psi'$  which we attribute to correlated non-charm 2e events such as Dalitz decays. We use these to determine a probability per hadronic event for such processes, and then extrapolate to calculate the expected contribution in the  $\psi''$  region. The numbers of events obtained are shown in Table II:

Table II

<u>Beam Energy</u>	<u>Observed 2e Events (resulting from selection + hand scan + cuts)</u>	<u>Two-Photon Background</u>	<u>Hadron Mis-Ident. Background</u>	<u>Correlated 2e Background</u>	<u>Signal (after background subtractions)</u>
resonant ( $\psi + \psi'$ )	14	$\ll 1$	7.8	6.4	0
non-resonant ( $E_{\psi} < E < E_{\psi'}$ )	2	0.5	0.8	0.6	
$D\bar{D}$ resonance ( $\psi''$ )	21	0.4	3.2	1.0	16.4

To determine the branching fractions, we relate the number of observed events to the number of  $D\bar{D}$  pairs which were produced multiplied by the detection efficiency and the probability to decay to electrons. For the 1e sample the observed number is approximately

$$(6) \quad N_{1e} = 2N_0 \epsilon_1^0 b^0(1-b^0) + 2N_+ \epsilon_1^+ b^+(1-b^+)$$

where  $N_0(N_+)$  = the number of neutral (charged)  $D\bar{D}$  pairs produced in the experiment.

and  $\epsilon_1^{0,+}$  = the probability to detect a 1e event from a  $D^0\bar{D}^0$  ( $D^+\bar{D}^-$ ) initial state in which one of the D mesons decays to an electron

and  $2b(1-b)$  is the probability that one D decays and the other doesn't.

In the 2e sample, the equation is similar but  $b^0$  and  $b^+$  are squared, since both must decay:

$$(7) \quad N_{2e} = N_0 \epsilon_2^0 b^{02} + N_+ \epsilon_2^+ b^{+2}$$

The efficiencies,  $\epsilon_2$ , are to detect a 2e event wherein both D mesons decay, and all these efficiencies include the effects of the cuts. In an ideal world these equations describe a line and ellipse in  $b^0, b^+$  space, as shown in Fig. 4. In actuality, the 1e line has a small curvature (due to the quadratic piece in equation 6 and also due to a small correction for cases in which both Ds decay, but only 1e is observed). In addition, since the observed events have statistical uncertainties associated with them, the lines actually broaden to regions whose edges correspond to the nominal data plus or minus the statistical uncertainty. The data is shown in Fig. 5, where two extreme possibilities are shown for assumptions regarding the decay of the D into  $K_{ev}$  versus  $K^*_{ev}$ . The above efficiencies are in fact averages over all possible semileptonic decay modes, and Fig. 5 demonstrates that the two regions of overlap are approximately independent

of the  $K$  versus  $K^*$  question, and furthermore that only two solutions are allowed: either  $b^0 \gg b^+$ , or  $b^0 \ll b^+$ .

It is possible that there is a statistical fluctuation which has led to overabundance of  $2e$  events, but to evaluate this, one can compare the probability of observing 21 or more events given the hypothesis that the branching ratios are equal. From Table III, using the world average semileptonic branching ratio<sup>8</sup> we would expect to observe only  $\sim 11$  events at a probability of  $\sim 4 \times 10^{-3}$ , which should be compared to a probability of roughly 50% to predict and observe 21. Thus it is extremely unlikely that the above observation is a fluctuation. Another explanation may be that there may be a miscalculation of the background such that not enough of the 21  $2e$  events are attributed to non-charm processes. As a separate check, one could assume that the background sources have two origins, one due to hadronic events (misidentification and Dalitz decays, for example) and the other due to luminosity (two-photon processes). Using this hypothesis to account for the background below the  $\psi''$  produces a smaller estimate of the background at the  $\psi''$  than the more detailed calculation.

To determine which of the two solutions allowed by Figure 5 is correct, we make use of the  $K_S^0$  content in the data, which is expected to come primarily from  $D^+ \rightarrow K^0 e^+ \nu$  decays. To get a feeling for the sensitivity of this technique, we show in Table IV the number of  $K_S^0$  we expect to detect depending on their origin. To isolate  $K_S^0$  candidates, we visually scan  $2e$  events for prongs coming from  $K_S^0$  decays which do not point back to the event origin in the azimuthal view. A Monte Carlo simulation indicates that typically only one detached track ("V") is observed from each  $K_S^0$ , since the other prong either misses the detector or aligns with the event vertex.



Table III

<u>branching ratio (<math>b^0=b^+</math>)</u>	<u>predicted 2e events (including background)</u>	<u>probability to observe 21 or more</u>
8.0%	10.8	$4 \times 10^{-3}$
9.0%	12.5	$16 \times 10^{-3}$

Table III. Probability to observe  $\geq 21$  events when  $b^0=b^+$  is assumed.

The current world average for b.r. ( $D \rightarrow Xev$ ) is 8%, (9% is  $+1\sigma$ ).

Table IV

<u>Process</u>		<u>Fraction of <math>K^0</math></u>	<u>Predicted Events (including 21 background events)</u>
$D \rightarrow K e \nu$ (100%)	$D^0 \rightarrow K^- e^+ \nu$	No $K^0$	2.6
	$D^+ \rightarrow K^0 e^+ \nu$	100% $K^0$	7.9
$D \rightarrow K^* e \nu$ (100%)	$D^0 \rightarrow K^0 \pi^- e^+ \nu$	67% $K^0$	3.8
	$D^0 \rightarrow K^- \pi^0 e^+ \nu$		
	$D^+ \rightarrow K^0 \pi^0 e^+ \nu$	33% $K^0$	3.7
	$K^+ \pi^- e^+ \nu$		

(Figure 6 shows the inner PWC tracks of two of the  $K_S^0$  candidate events.)

Of the 21 2e events, 8 have a "V". Immediately, two conclusions are obvious (pending a discussion of the backgrounds in the 2e+V sample):

First, the only decay mode that can produce enough 2e+V events comes from  $D^+D^-$  events (hence  $b^+ \gg b^0$  is the solution) and second,  $D^\pm \rightarrow Kev$  is favored over  $D^\pm \rightarrow K^*ev$ .

The background to the 2e+V events consists of false V's with either real or false electrons, or real V's with false electrons. False V's result from particle interactions in the beam pipe, or from in-time cosmic rays which traverse only part of the cylindrical chamber. Additional false V's will originate in charged K decays which occur before the cylindrical PWC. The probability of a false V (of non-charm origin) is determined by scanning  $\psi' \rightarrow \psi\pi^+\pi^-$  events to obtain the fraction of such events which  

$$\begin{array}{l} \psi' \rightarrow \psi\pi^+\pi^- \\ \quad \downarrow \\ \quad e^+e^- \end{array}$$
exhibit a detached track. The first background is then determined by the product of the 21 2e events multiplied by the false V probability, with an additional small correction (calculated by Monte Carlo) for  $K^\pm$  decays in flight. The second background similarly is the product of the 4.6 2e background events multiplied by the probability of a real V, which is obtained by a study of the 1e + V events at the  $\psi''$ . After subtracting these backgrounds, we find that 5.9  $D\bar{D}$  events contain 2 electrons and a detected  $K_S^0$ , as shown in Table V.

Table V

	Observed Events	
	<u>2e</u>	<u>2e+V</u>
Total	21	8
Background	4.6	2.1
Signal	16.4	5.9

From the relative abundance of  $K_S^0$  events, we conclude that the upper left solution of Figure 5 is excluded, leaving the problem of extracting the branching ratios allowed by the triangular region in the lower right. To do this, we form a statistical likelihood  $L(b^0, b^+)$  which is the product of probabilities to observe three quantities: 1) the number of 1e events, for which we use a Gaussian probability density  $P_{1e} = \exp^{-\frac{1}{2}} \left( \frac{N_{1e} - M_{1e}}{\sigma_{1e}} \right)^2$  where  $N_{1e}$  is the predicted number of 1e events as given by equation 6, and  $M_{1e}$  is the measured number. 2) The number of 2e events, for which we use a Poisson probability density

$$P_{2e} = \frac{(N_{2e})^{M_{2e}} e^{-N_{2e}}}{M_{2e}!} \text{ where } N_{2e} \text{ is the number of 2e events predicted by}$$

equation 7 (plus background) and  $M_{2e}$  is the measured number of 2e events.

3) The number of 2e+V events, using a Poisson probability density, but renormalized to an observed signal of 16.4 2e events to remove the obvious correlation between 2e and 2e+V events.

One difficulty with this calculation is that it depends (to the extent shown by Fig 5) on the ratio  $r_K = \Gamma(D \rightarrow Kev)/\Gamma(D \rightarrow Xev)$ . This ratio has been determined at DELCO by making use of the electron momentum spectrum<sup>6</sup>, which favors stiffer electrons for the  $D \rightarrow Kev$  decay. The measured spectrum has been fit to a mixture of decay modes:  $(D \rightarrow \pi ev) + (D \rightarrow Kev) + (D \rightarrow (K\pi)ev)$ , where the  $(K\pi)$  system is either non-resonant or resonant  $K^*(890)$ . The result is that  $D \rightarrow Kev$  accounts for a contribution of  $55 \pm 14\%$  if the  $K\pi$  system is resonant, and  $38 \pm 19\%$  if the  $K\pi$  is non-resonant. From the large number of 2e+V events, the data favors the rate for  $D^+ \rightarrow Kev$  as large as possible. Fig. 7a shows the probability density as a function of  $r_K$  from the 1e momentum spectrum determination, where the two possibilities have been drawn to

have the same height. The probability density for  $r_K$  as calculated from the  $2e+V/2e$  ratio is shown in Figure 7b. If one uses the dashed curve of Fig. 7a as an estimate that includes the ambiguity in the  $1e$  result, and combines the curve of 7b with it, the result is depicted in Figure 7c - from which one concludes that  $r_K$  is approximately  $.55^{+.15}_{-.30}$ .

There is an additional measurement<sup>3)</sup> from the tagged D sample of the Mark II collaboration, which indicates that  $r_K = 0.68 \pm 0.28$ . Thus, for purposes of the likelihood function, we use  $r_K = 0.60$  and include a variation of  $\pm 0.2$  in the estimate of systematic uncertainties.

The remaining difficulty with the likelihood method is the difficulty of estimating systematic uncertainties which do not cancel between equations 6 and 7. The largest of these are the integrated luminosity, Cherenkov efficiency, and neutral/charged fraction. To estimate their effects, we have allowed the variations to range between their extreme values, but have included the probability of such an excursion into the likelihood function, which becomes the product of probabilities to observe  $1e$ ,  $2e$  and  $2e+V$  events (when the predicted number includes a systematic variation) multiplied by the probability that the variation will occur. We plot in Figure 8 equal probability contours in  $b^0$  and  $b^+$  corresponding to  $\chi^2$  variations of 1 and 4 where  $\chi^2 = -2 \ln L(b^0, b^+)$  and both statistical and systematic effects have been included. The result lies near the edge of the physical region for  $b^0$ , thus we quote an upper limit  $b^0 < 4.0\%$  (95% CL) and an independent result:  $b^+ = (22.0^{+4.4}_{-2.2})\%$ . The minimum value for the ratio along the  $2\sigma$  contour occurs at about  $b^0 = 4\%$ ;  $b^+ = 16\%$  so that  $R(b^+/b^0) > 4.3$  (95% CL).

Isospin symmetry predicts that both  $D^0$  and  $D^\pm$  semileptonic rates

should be nearly equal, so this measurement implies that the total lifetimes also differ by the ratio  $\tau_{D^+}/\tau_{D^0} > 4.3$ . The lifetime may be calculated from a well-understood theoretical rate<sup>9</sup>  $\Gamma(D \rightarrow K\pi) = (1.1 - 1.4)10^{11} \text{ sec}^{-1}$  where the range comes from various estimates of the form factor. Using the data for the branching fractions and  $r_K$  together with the theoretical rate  $(1.4 \times 10^{11}) \text{ sec}^{-1}$  gives  $\tau_{D^0} < (2.2) \times 10^{-13} \text{ sec}$  and  $\tau_{D^+} = (12 \pm 5) \times 10^{-13} \text{ sec}$ .

From the Mark II detector, the ability to fully reconstruct simple hadronic final states from D decays allows identification of the charge nature of the  $D\bar{D}$  pair<sup>3</sup>. For their inclusive analysis, the  $K^-\pi^+$  and  $K^-\pi^+\pi^+\pi^-$  modes are used to identify  $D^0$  decays, and  $K^-\pi^+\pi^+$  and  $K^0\pi^+$  are used for  $D^+$  decays. These channels are relatively free of background, and one can examine the remainder of the event for electrons to determine the branching ratios. The experimental backgrounds have several origins, the most important of which are hadrons misidentified as electrons and falsely tagged events. (The smaller sources are  $\gamma$  conversions and Dalitz decays as well as charged K decays in flight). The hadron misidentification problem leads to the observation of events with electrons having the wrong sign opposite the tag. (A "wrong sign" electron has the opposite sign to the kaon observed in the tagged D.) The misidentified hadrons are removed using a measured misidentification probability to calculate the number of background events, which in turn is observed to be consistent with the observed wrong sign background.

The falsely tagged events are those lying within the reconstructed D mass region which are not D's. The contamination is small, and is removed by comparison of the rates within sideband mass regions. The observed

Table VI

<u>Decay Mode</u>	<u>#Tags</u>	<u>Net Events (After Bkgd Corrections)</u>	<u>Branching Ratios(%)</u>
$D^+ \rightarrow e^+$	$295 \pm 18$	$23.3 \pm 6.7$	$16.8 \pm 6.4$
$D^0 \rightarrow e^+$	$477 \pm 23$	$12.3 \pm 7.6$	$5.5 \pm 3.7$

number of events is summarized in Table VI. Using a maximum likelihood fit to the observed quantities, the Mark II collaboration obtains the ratio of branching fractions  $R(b^+/b^0) = 3.08^{+4.1}_{-1.3}$  where the quoted errors are statistical. Including an estimate of systematic uncertainties reduces this result to  $R(b^+/b^0) = 3.1^{+4.2}_{-1.4}$ .

In addition to the results from SPEAR, there is a direct measurement of the proper time distribution of D decays produced in  $\nu$  interactions.<sup>10</sup> This experiment measures the lifetime(s) directly by reconstructing the D decay within a very high resolution emulsion target. Since a detailed report of this experiment has been given at this conference<sup>11</sup>, I will conclude with a comparison of the results as shown in Table VII.

Since the discovery that the  $D^0$  and  $D^+$  do not have the same lifetime, there has been considerable effort and confusion in the attempts to incorporate the experimental measurements into a theoretical framework. The first point to be made is that there is relative confidence in the calculation for the semileptonic rates<sup>9</sup> (there is only one diagram, Fig. 9) and therefore the lifetime difference must originate in the non-leptonic part of the Hamiltonian. The literature is already voluminous, with attempts underway to incorporate the lifetime difference into the light spectator quark framework as well as to generate new phenomenological predictions for other charm non-leptonic decays. One of the initial observations is that the contribution from W exchange diagrams can enhance the non-leptonic rate for  $D^0$  decays but do not exist for  $D^+$  (Fig. 10). If the role of W exchange dominance turns out to be important, then one expects similar rate differences to occur in B meson decays, and in particular that the neutral B meson will be more difficult to detect via the decay  $B^0 (b\bar{d}) \rightarrow \psi\bar{K}\pi$  than will the charged one.<sup>12,13</sup>



Table VII

<u>Experiment</u>	<u><math>\tau_{D^0}</math> (sec)</u>	<u><math>\tau_{D^+}</math> (sec)</u>	<u><math>R(\tau^+/\tau^0)</math></u>
DELCO	$<2.2 \times 10^{-13}$ (95%CL)	$12 \pm 5 \times 10^{-13}$	$>4.3$ (95%CL)
Mark II	$(3.7 \pm 2.8) \times 10^{-13}$	$(11.2 \pm 5.1) \times 10^{-13}$	$3.1^{+4.2}_{-1.4}$ ( $\lambda 0.6$ at 95%CL)
FNAL E531	$(0.93^{+0.52}_{-0.29}) \times 10^{-13}$	$(10.0^{+8.9}_{-4.6}) \times 10^{-13}$	10.75

The E531 results are preliminary, with more events expected (see ref. 11).

The Mark II results are from ref. 3.

In conclusion, the results from  $e^+e^-$  annihilations have shown that the semileptonic branching ratios are different for neutral and charged D mesons, which implies that their lifetimes are also unequal. Experimental confirmation of the lifetime difference is provided by the  $\nu$ -emulsion measurement and all three experiments seem to be in reasonable agreement. The theoretical challenge is how to develop calculational techniques for the non-leptonic Hamiltonian which account for the D lifetime difference, and can be subjected to further tests in the decays of charmed and bottom particles.

1. N. Cabibbo and L. Maiani, Phys. Lett. 73B (1979) 418.
2. Preliminary results were presented by J. Kirkby, Proceedings of the International Symposium on Lepton and Photon Interactions at High Energies, Fermilab, Batavia, Illinois, 1979.
3. R. Schindler, Ph.D. thesis, Stanford University, SLAC Report 219 (1979) unpublished.
4. M. Katuya, Iowa State preprint 79-0882, 1979.
5. W. Bacino et al., Phys. Rev. Lett. 40, 671 (1978).
6. W. Bacino et al., Phys. Rev. Lett. 43, 1073 (1979).
7. R. Bhattacharya, J. Smith, and G. Grammer, Phys. Rev. D15, 3267 (1977).  
J. Smith, J.A.M. Vermaseren, G. Grammer, Phys. Rev. D15, 3280 (1977).  
J.A.M. Vermaseren, J. Smith, G. Grammer, Phys. Rev. D19, 137 (1979).
8. The source for the most current world average for D semileptonic branching ratios is ref. 2.
9. D. Fakirov and B. Stech, Nucl. Phys. B133, 315 (1978).
10. J. Prentice, Proceedings of the International Symposium on Lepton and Photon Interactions at High Energies, Fermilab, Batavia, Illinois, 1979.
11. N. Reay, private communication and Proceedings of this Conference.
12. R. Heinze, Proceedings of this Conference.
13. For a theoretical discussion of W exchange dominance in B decay, see S. P. Rosen, Purdue preprint 80-0220, 1980.

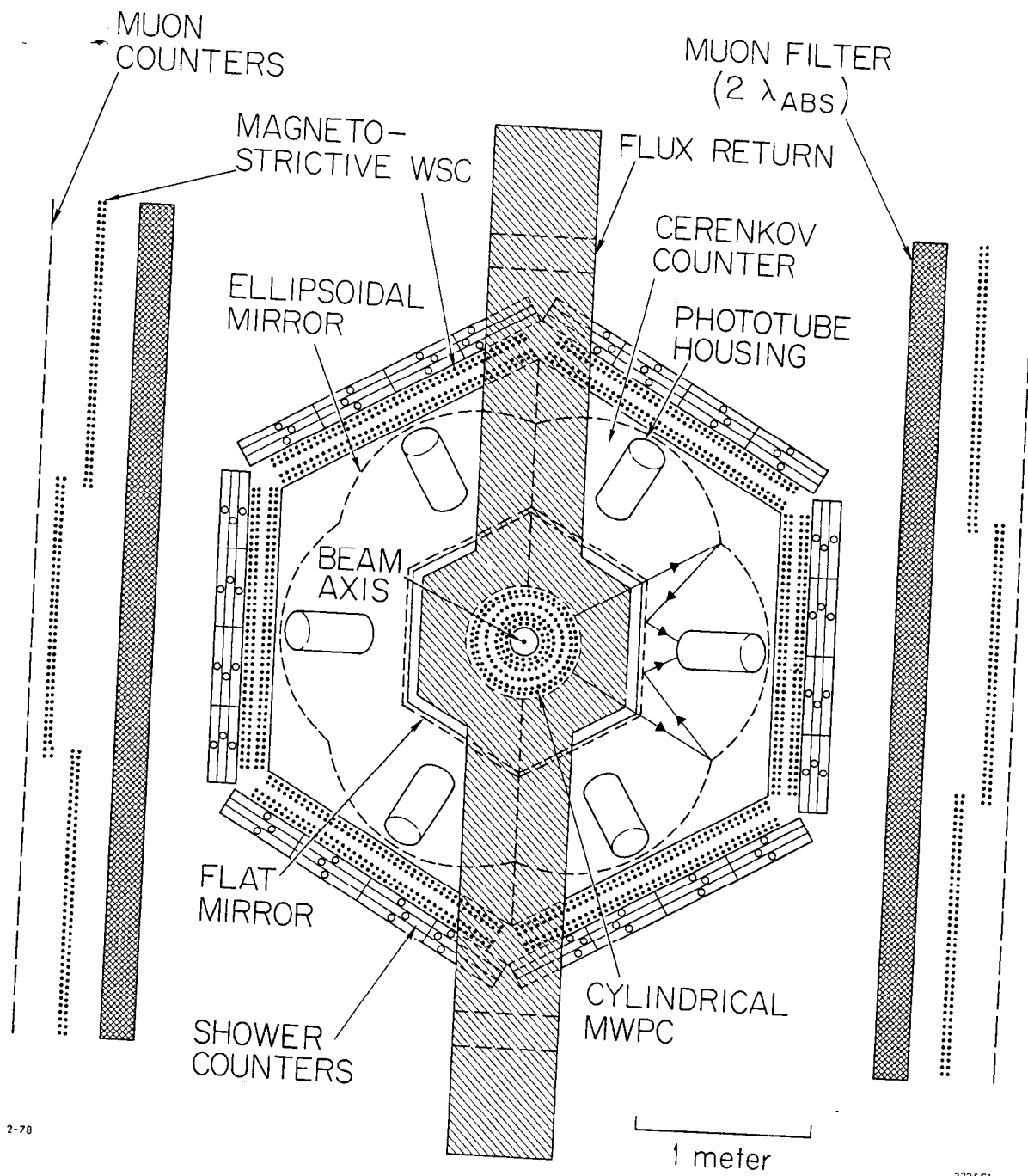
Figure Captions:

1. (a) Polar and (b) azimuthal projections of the apparatus. For illustrative purposes, in (a) the apparatus in the yoke has been rotated by  $30^\circ$ .
2. The electron momentum spectrum of the multiprong 2-electron events observed at the  $\psi''$ . The curve indicates the charm spectrum observed in the 1-electron events.
3. Two-photon processes which produce spurious multiprong 2-electron events.
4. Idealized solutions for  $b^0$  and  $b^+$  given the observed numbers of multiprong 1-electron and 2-electron events from charm decays.
5. The values of  $b^0$  and  $b^+$  as obtained from the data which correspond to  $\pm 1\sigma$  statistical variations in the observed number of 1-electron and 2-electron events. The data are shown under two extreme assumptions for the detection efficiencies: (a) all semileptonic D decays occur as  $D \rightarrow K e \nu$ ; (b) all semileptonic D decays occur as  $D \rightarrow K^* e \nu$ .
6. Azimuthal projections of the inner PWC tracks for two  $K_S^0$  candidate events from the multiprong 2-electron sample.
7. (top) Probability density as a function of  $r_K$  (defined in text) for the hypothesis  $D \rightarrow K^* e \nu$  and  $D \rightarrow (K\pi) e \nu$  (non-resonant) as determined from a fit to the electron momentum spectrum in the multiprong 1-electron sample. (see ref 6.) The dashed line is a hand-drawn representation of the probability density allowing for the possibility that either hypothesis could be true.

(middle) Probability density as determined by the  $2e+V/2e$  ratio in the multiprong 2-electron events. Two limiting possibilities ( $b^+/b^0 = \infty$ , and  $b^+/b^0 \geq 4$ ) define the shaded region.

(bottom) Combined probability density using both determinations.

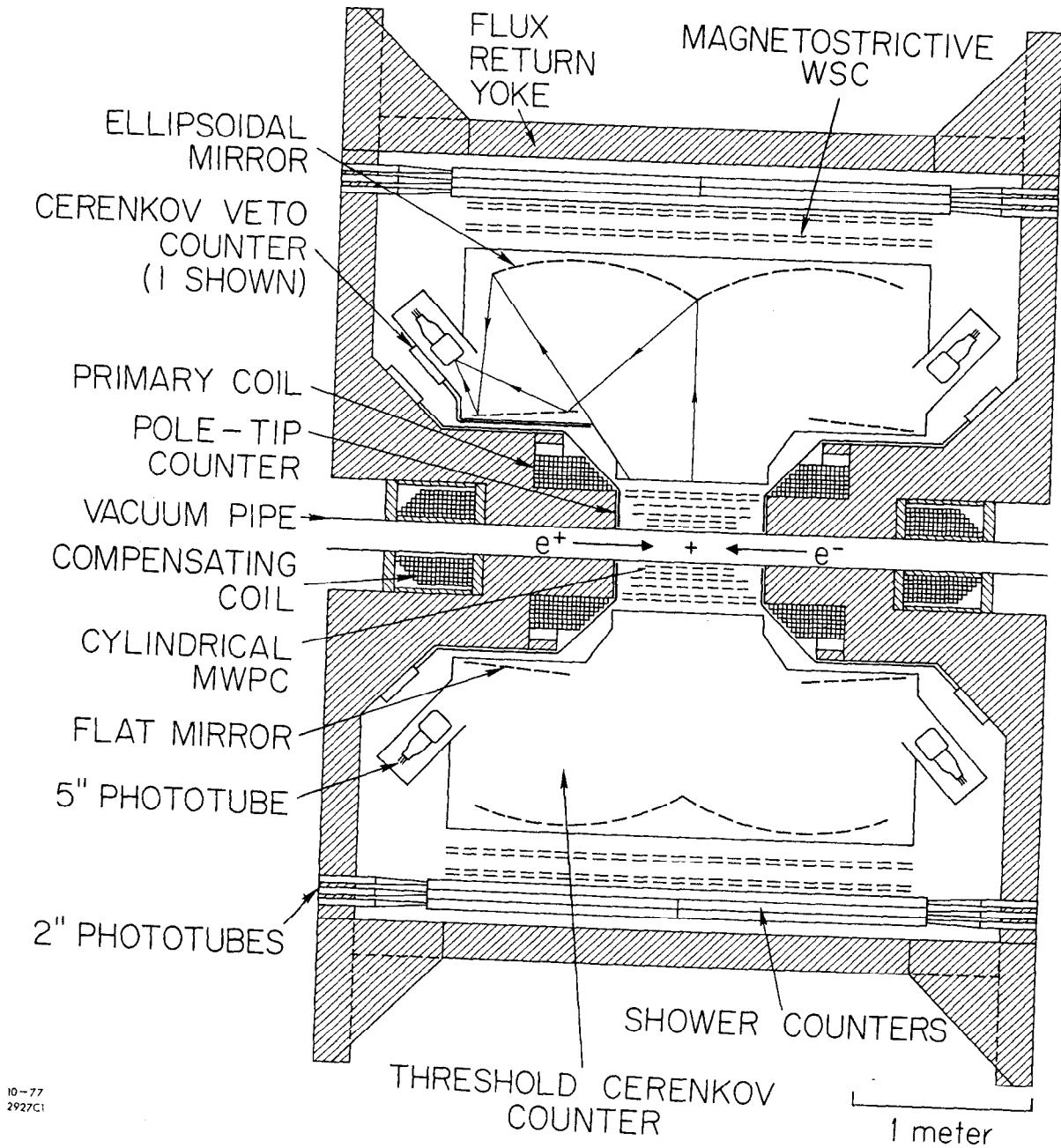
8. Probability contours corresponding to  $\chi^2$  changes of 1 and 4 ( $1\sigma$  and  $2\sigma$  in  $b^0$  and  $b^+$ , independently) calculated from the likelihood function for observing the measured number of  $1e$ ,  $2e$  and  $2e+V$  events. Both the statistical and systematic uncertainties have been included.
9. W-radiation diagram for D semileptonic decays.
10. W exchange diagram for  $D^0$  decays, which does not exist for  $D^+$  decays.



2-78

3225C1

Fig. 1a



10-77  
2927C1

Fig. 1b

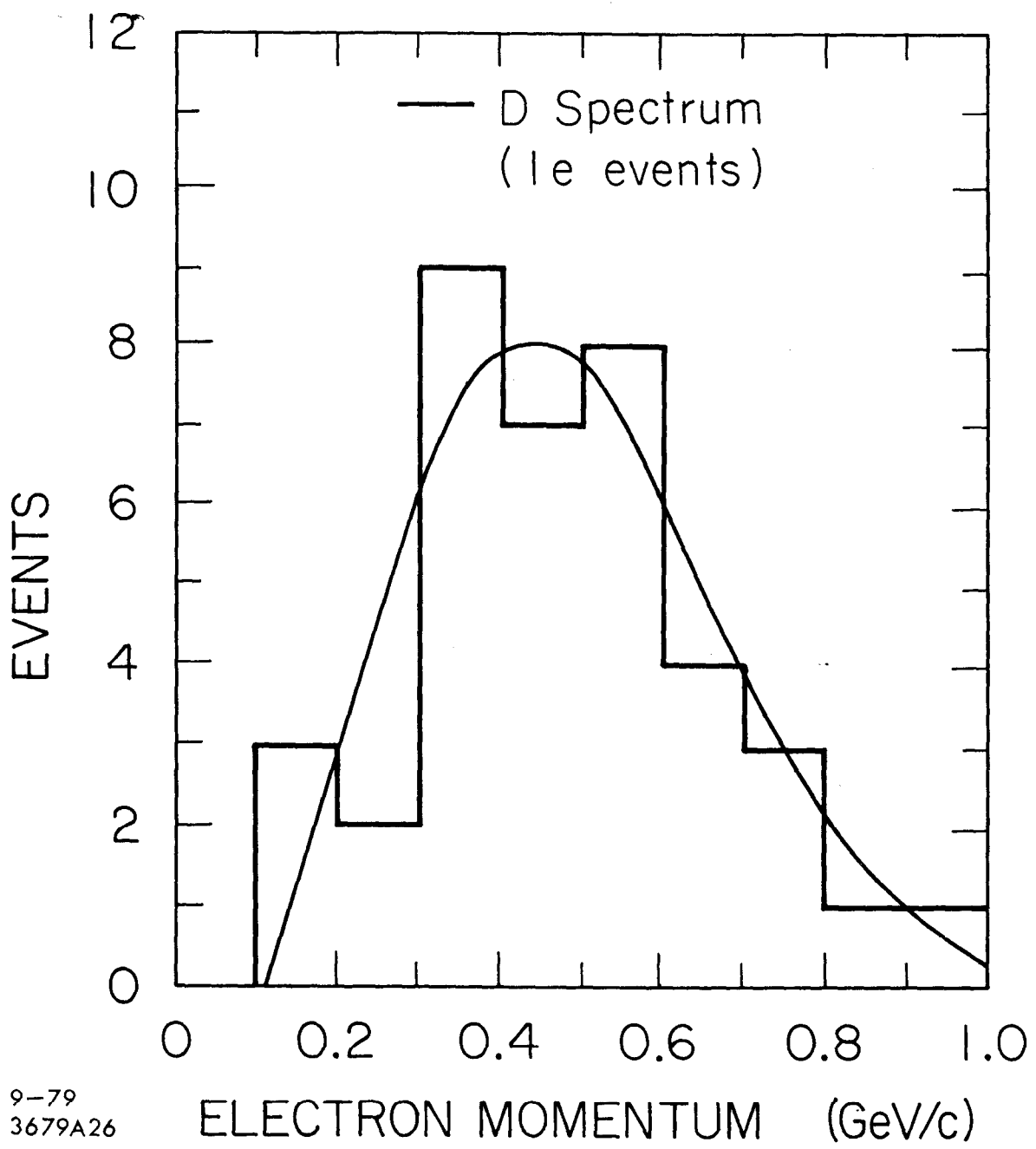
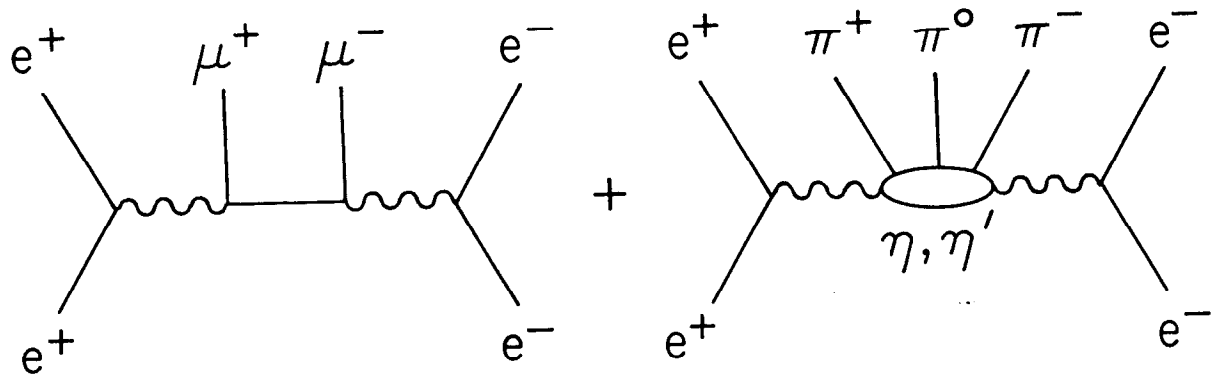


Fig. 2





4-80

3773A5

Fig. 3

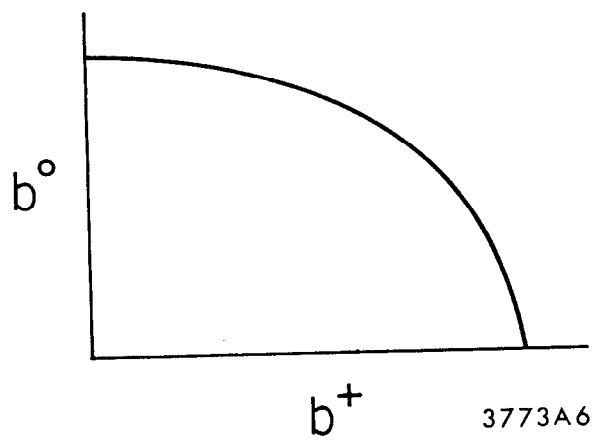
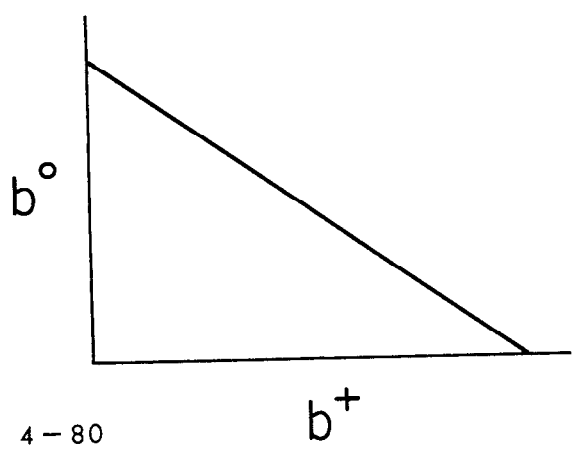


Fig. 4

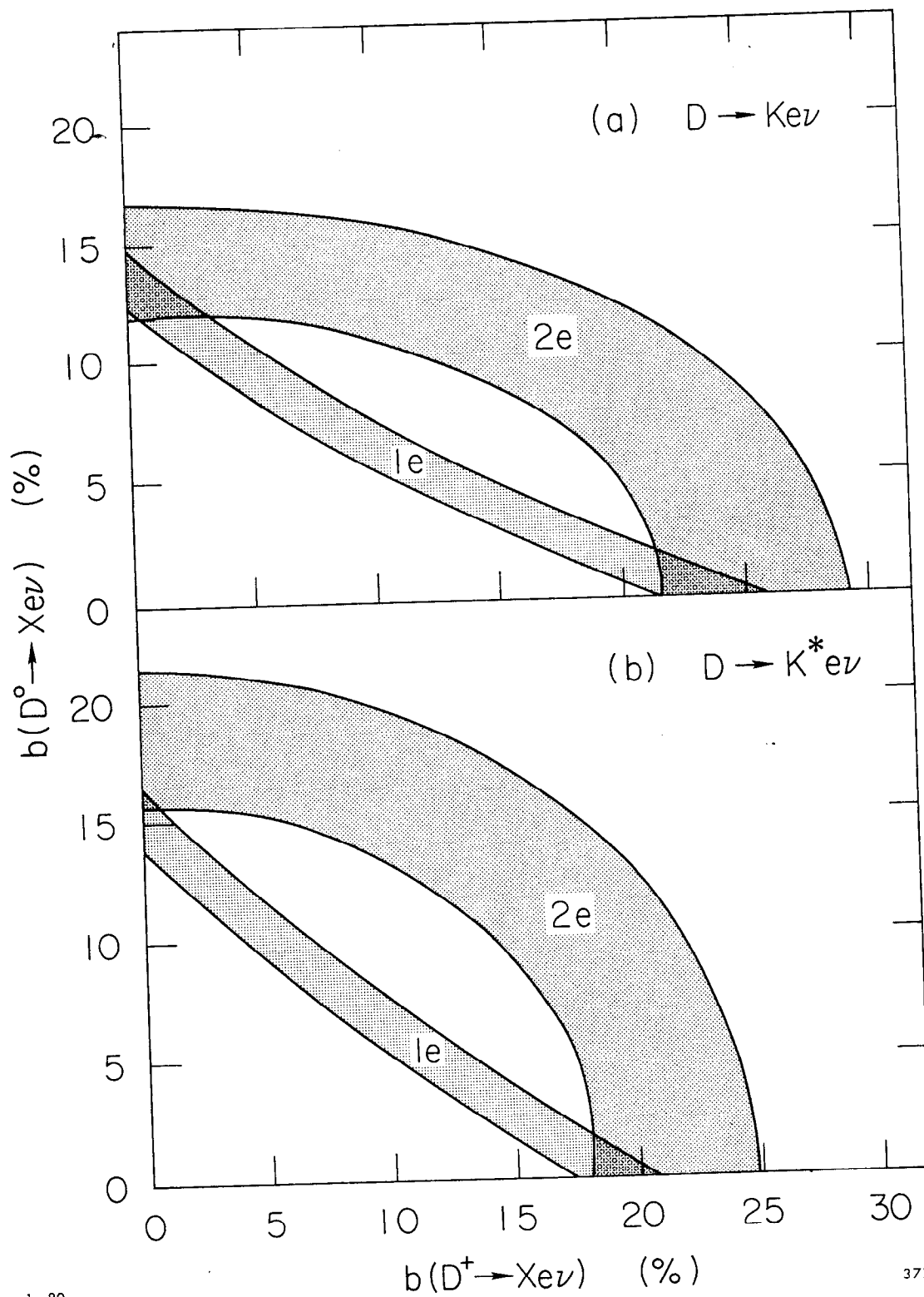
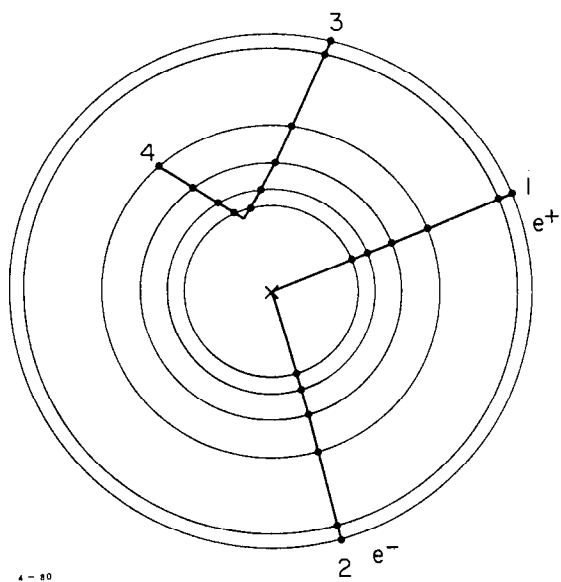


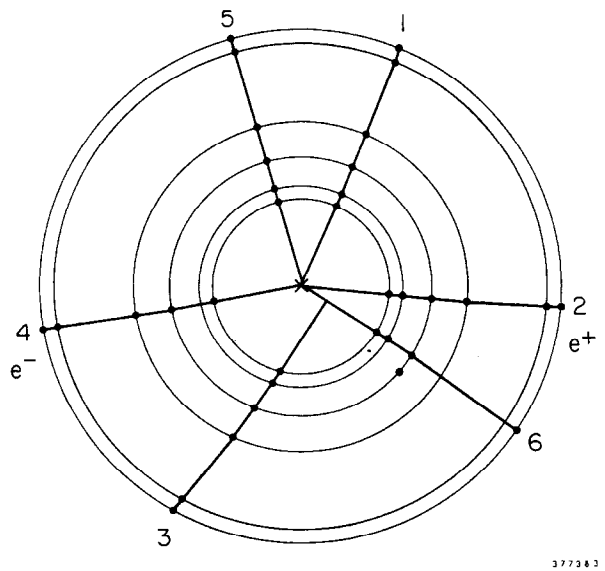
Fig 5

RUN EVENT ENERGY  
2299 673 1.89



4-80

RUN EVENT ENERGY  
545 13124 1.89



377383

Fig. 6

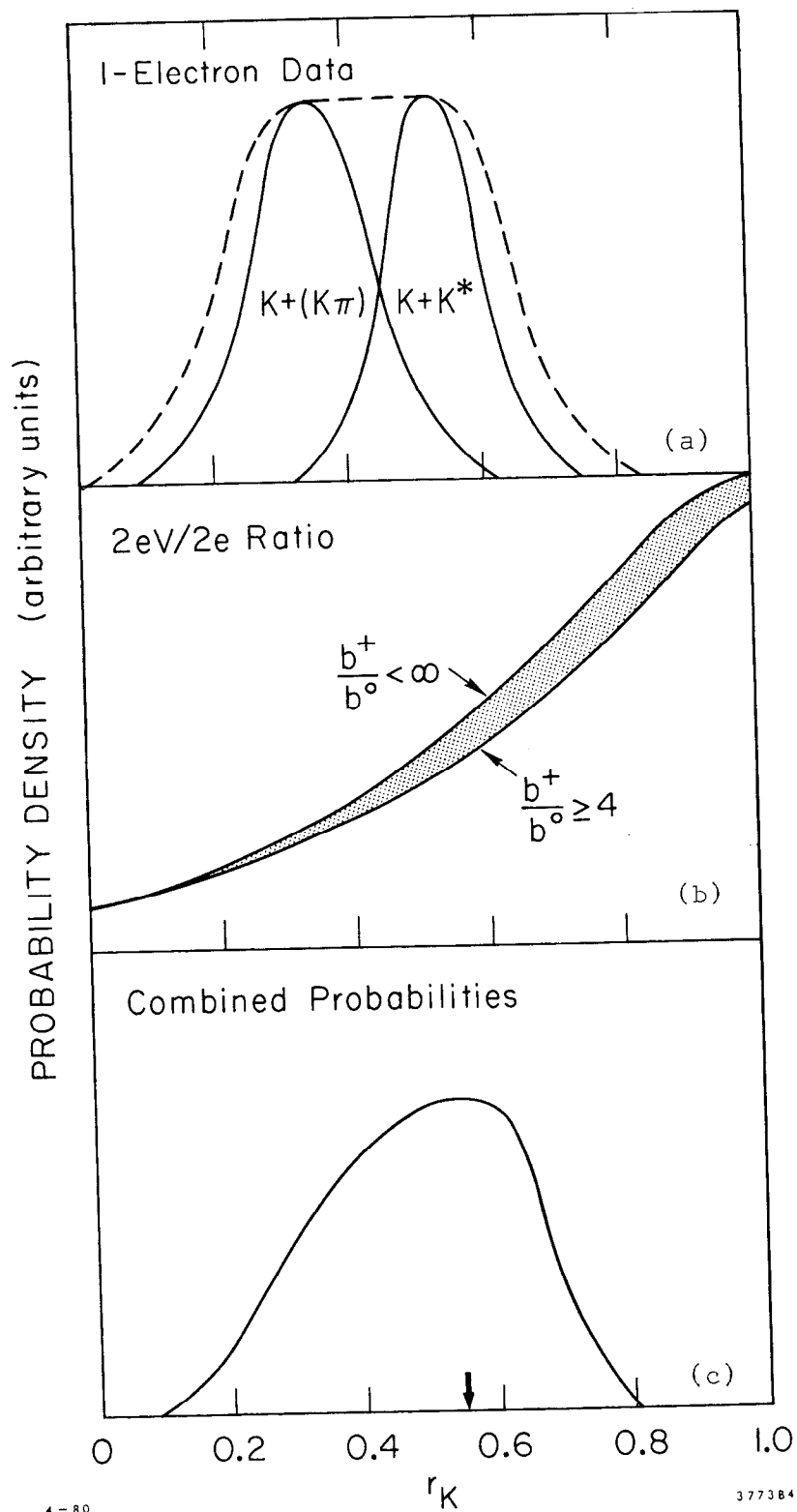


Fig. 7

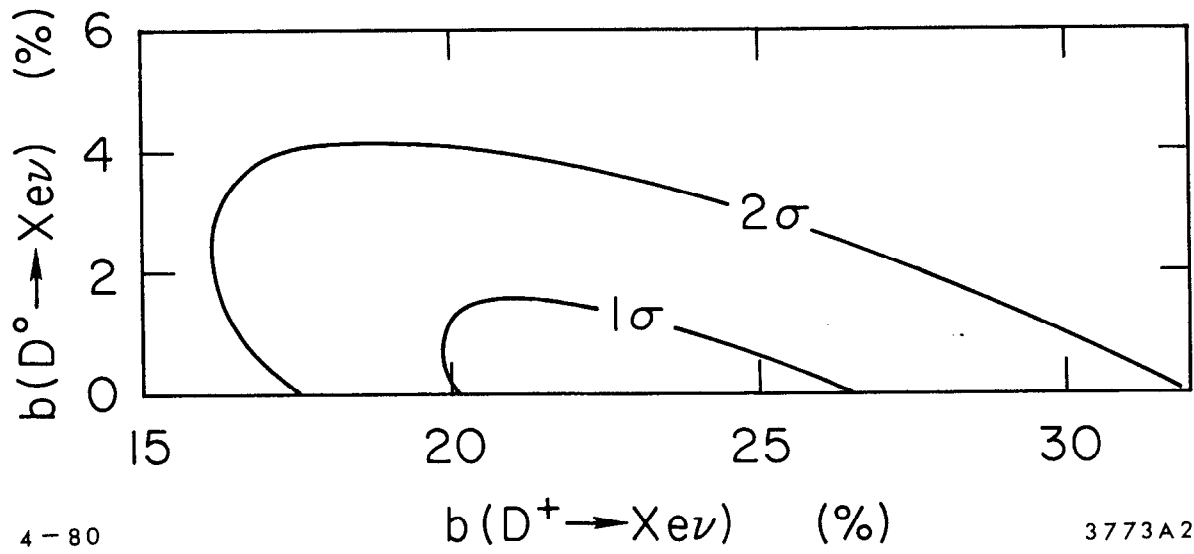


Fig. 8

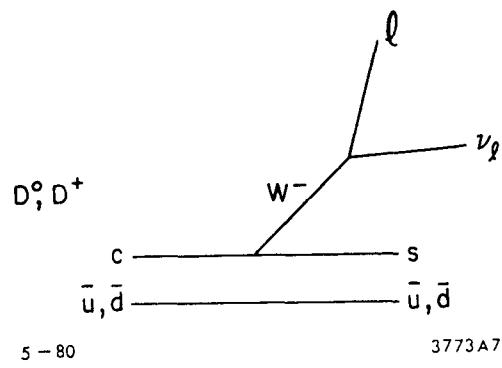


Fig. 9

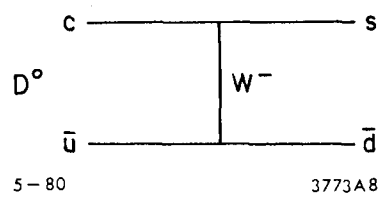


Fig. 10